Two-Dimensional Pulsed EPR Studies of Vanadium-Exchanged ZSM-5

James Woodworth,[†] Michael K. Bowman,[‡] and Sarah C. Larsen*[,†]

Department of Chemistry, University of Iowa, Iowa City, Iowa 52242, and Environmental Molecular Sciences Laboratory, Pacific Northwest National Laboratory, Richland, Washington 99352

Received: July 30, 2004

The pulsed electron paramagnetic resonance (EPR) technique of hyperfine sublevel correlation spectroscopy (HYSCORE) was used to obtain structural information about vanadium(VO^{2+})-exchanged ZSM-5. HYSCORE spectra were obtained for vanadium-exchanged ZSM-5 before and after dehydration and after the adsorption of ammonia. For the hydrated samples, proton hyperfine coupling constants were measured and assigned to equatorial water ligands with orientations perpendicular and parallel to the equatorial plane. Nitrogen hyperfine coupling constants for adsorbed ammonia were also determined from the HYSCORE spectra. The results were compared with previous density functional theory (DFT) calculations of hyperfine coupling constants for vanadyl model complexes.

Introduction

Vanadium-exchanged, -substituted, and -impregnated zeolites and mesoporous materials have been investigated as catalysts for use in applications such as emission abatement reactions and oxidation reactions.[1−6] Vanadium-exchanged zeolites are prepared by standard ion-exchange or vapor-phase procedures in which vanadyl ion (VO^{2+}) replaces the charge-compensating cation in the zeolite. In contrast, vanadium-substituted zeolites are prepared by introducing vanadium during the zeolite synthesis so that vanadium replaces silicon or aluminum in the tetrahedral framework sites. Whittington and Anderson studied toluene oxidation on vanadium-exchanged and -substituted zeolites and determined that the surface-bound VO^{2+} groups were responsible for the catalytic activity.[1] The vanadium-substituted zeolites showed more resistance to leaching relative to the vanadium-exchanged zeolites. Mesoporous matrials, such as MCM-41 and MCM-48, were impregnated with V_2O_5 and were subsequently evaluated for catalytic activity in the partial oxidation of methane to formaldehyde.[6] Vanadium incorporation into MCM-48 materials has also been investigated.[7]

In a recent study, Wark and co-workers demonstrated that vanadium-exchanged ZSM-5 (VO^{2+}−ZSM-5) is active for the selective catalytic reduction of nitric oxide with ammonia (SCR−NH_3).[5] The vanadium-exchanged zeolites were found to have catalytic activity comparable to that of V_2O_5/TiO_2, which is a commercial catalyst for SCR−NH_3 of NO_x in flue gases of stationary sources. One problem with V_2O_5/TiO_2 catalysts is that they are unstable at the high temperatures that are required for the SCR−NH_3 reaction. In contrast, vanadium-exchanged zeolite catalysts are very stable at elevated temperatures. The catalytic activity of VO^{2+}−ZSM-5 for SCR−NH_3 has been attributed to the VO^{2+} species with vanadium in the V^{4+} oxidation state.[5] However, very little direct spectroscopic information about the interaction of ammonia with the active vanadium species in vanadium-exchanged zeolites has been obtained.

The EPR spectrum for the vanadyl ion, VO^{2+}(V^{4+}, d^1), depends on the local electronic and ligand environments of the vanadium center. The continuous wave (CW) EPR spectrum for a rigid limit VO^{2+} system is dominated by the axial hyperfine interaction between the unpaired electron spin ($S = {}^1/_2$) and the ^{51}V nuclear spin ($I = {}^7/_2$, 99.8% natural abundance).[8] The parallel components of the vanadium **g** and hyperfine **A** tensors are sensitive to the ligand environment and the coordination of the vanadium center. The vanadium quadrupole coupling constant has also been shown to reflect the local electronic environment.[9,10] In previous studies of vanadium-exchanged and -substituted zeolites, the CW EPR spectra for vanadyl-exchanged zeolites have been used to determine the vanadium hyperfine and **g** values.[1−5,11−13] In these studies, the local symmetry of the vanadium center was determined after various pretreatment and reaction conditions. Recently, quantum chemical calculations of vanadium **g** values and hyperfine and quadrupole coupling constants have been used to interpret the EPR spectra for vanadium-exchanged zeolites.[10,14−18]

Metal ligand hyperfine coupling constants (A_L) are typically too small to be resolved in the CW EPR spectrum. The unpaired electron on the vanadium is primarily in a d_{xy} orbital; therefore, the overlap with the ligand orbitals is weak, leading to small values for the ligand hyperfine coupling constant. Experimentally, A_L values in vanadyl systems can be measured by pulsed EPR techniques such as electron spin−echo envelope modulation (ESEEM) or electron nuclear double resonance (ENDOR);[8,19−33] for example, ESEEM methods can be used to measure nitrogen isotropic hyperfine coupling constants (A_N) in the range of ∼1−10 MHz.[27,28,33] For ligand nuclei with $I > {}^1/_2$, the quadrupole coupling constants can also be measured and can provide additional information about the local electronic environment of the ligand.[28,30,33] In a study by Larsen and Singel, the nitrogen hyperfine and quadrupole coupling constants for ammonia adsorbed on silica-supported vanadium oxide were measured using ESEEM spectroscopy.[28] Standard ESEEM methods have been used extensively by Kevan and co-workers to obtain valuable distance information about coordinated ligands in transition-metal-exchanged zeolites.[4,11,34−43]

* Corresponding author. E-mail: sarah-larsen@uiowa.edu.
[†] University of Iowa.
[‡] Pacific Northwest National Laboratory.

10.1021/jp046585r CCC: $27.50
Published on Web 09/16/2004

Recently, a 2D ESEEM experiment, hyperfine sublevel correlation spectroscopy (HYSCORE),[44] has been widely used to investigate a range of biological and materials systems.[45−51] The advantage of the HYSCORE experiment relative to standard ESEEM methods is that spectral assignments are simplified because of cross peaks in the 2D spectrum that correlate nuclear frequencies from different electron spin manifolds, simplifying spectral assignments[52] and decreasing spectral overlap. For hyperfine interactions with nuclei having no or negligible nuclear quadrupole interactions, the cross peaks that correlate frequencies involving the same nucleus take the form of arcs.[50,53,54] The curvature of these arcs is caused by a second-order shift that can be used to estimate the dipolar part of the hyperfine interaction. Previously,[50,54] it was shown that the curved arcs in the experimental spectrum are transformed into straight lines by a simple change of coordinates. The resulting straight lines are readily fit by linear regression methods to yield the principal values of the hyperfine tensor even in the case of nonaxial tensors. This approach has been used with great success for protons even when only a limited portion of the HYSCORE arc can be measured.[53,55] Strong modulation from other nuclei, such as nitrogen, often make it impractical to use acquisition parameters that produce the maximum extent of the proton cross peaks. However, coordinate transformation combined with linear regression can recover the full proton hyperfine tensor from a single HYSCORE spectrum and can be used to combine data from several HYSCORE measurements with different acquisition parameters. Incomplete arcs are also common under conditions of orientation selection, that is, when **g**-tensor or hyperfine-tensor anisotropy prevents the simultaneous measurement of signals from all possible orientations. The limited range of orientations that can be measured often includes only a part of the full range of hyperfine couplings. Orientation selection is a typical feature with metal centers such as vanadium. Again, the coordinate transformation method allows for the analysis of the short sections of cross peaks that result from orientation selection and also offers a way of combining data that is measured at different magnetic fields to extend the range of orientations represented in the data.[53]

In this study, HYSCORE spectroscopy is used to elucidate the structure of hydrated VO^{2+}-exchanged ZSM-5 through the analysis of the proton nuclear frequencies. The interaction of the VO^{2+}-exchanged ZSM-5 with ammonia was also investigated using HYSCORE spectroscopy, providing detailed structural information about the hydrated and ammonia complexes. The implications of these findings for catalysis are also discussed.

Experimental Section

Sample Preparation. Vanadium-exchanged ZSM-5 was prepared from a commercial sample of NaZSM-5 (Zeolyst, Si/Al = 16) via an aqueous exchange procedure using approximately 5.0 g of the parent zeolite in 200 mL of 0.05 M $VOSO_4$. The mixture was stirred overnight at room temperature, filtered, washed with 1.0 L of deionized water, and then dried overnight in an oven at 330 K. This process was repeated twice for ZSM-5 to achieve a higher level of exchange.

The vanadium-exchanged ZSM-5 was characterized by ICP-AES (inductively coupled plasma atomic emission spectroscopy) using a Perkin-Elmer Plasma 400 for elemental analysis. The sample was analyzed to determine the Si/Al ratio and the vanadium loading. The form of sample identification that will be used throughout this paper is zeolite − Si/Al ratio − exchange level (%) (i.e., VO^{2+}−ZSM5 −12 − 24 has Si/Al = 12 and a vanadium exchange level of 24%). The exchange level was calculated by taking the V/Al ratio from the ICP results and multiplying by 2 to account for the theoretical exchange of two Al atoms for every 1 VO^{2+} ion (2 × (V/Al) × 100% = % V exchange). The sample used in this study was VO^{2+}−ZSM5 − 16 − 38, corresponding to a vanadium weight percent of 0.87%.

The treatment of the samples was carried out in 4-mm EPR tubes that were fit with high-vacuum valves. Ammonia was adsorbed onto the ZSM-5 sample by first evacuating the sample tubes and then exposing the sample to 250 Torr of anhydrous ammonia for 30 min, yielding an equilibrium pressure of 150 Torr. The sample was then evacuated for 10 min and was sealed under vacuum. Fresh or air-exposed samples are referred to as hydrated.

HYSCORE Spectroscopy. HYSCORE spectroscopy is a four-pulse 2D electron spin−echo envelope modulation (ESEEM) experiment. The HYSCORE experiments were preformed with an X-band Bruker ESP 380E spectrometer. HYSCORE spectra were acquired using the four-pulse sequence ($\pi/2 - \tau - \pi/2 - t_1 - \pi - t_2 - \pi/2 - \tau -$ echo) and a four-step phase cycle to eliminate unwanted echoes.[56] The pulse widths, τ values, and experimental conditions for each spectra are listed in the figure captions. Data were processed using Bruker 2D WIN-EPR software. Each spectrum was baseline corrected, zero filled to 2^{10} points, and apodized using either a Gaussian or trapezoidal window function prior to being Fourier transformed in two dimensions into magnitude spectra 512 × 1024 points.

Results and Discussion

HYSCORE Spectral Features. In the HYSCORE experiment for an $S = 1/2$, $I = 1/2$ system, the nuclear spin transitions of one electron spin manifold (α) are correlated with the nuclear spin transitions of the other electron spin manifold (β) such that the correlations appear as off-diagonal cross peaks at (ν_α, ν_β) and (ν_β, ν_α) in the 2D spectrum. For an axially symmetric spin system, the principal values of the hyperfine tensor, **A**, are ($A_\perp$, $A_\perp$, $A_{||}$) where $A_\perp = A_{iso} - T$ and $A_{||} = A_{iso} + 2T$; A_{iso} and T are the isotropic and anisotropic hyperfine coupling constants, respectively. The nuclear frequencies for an axially symmetric spin = 1/2 nucleus coupled to a spin = 1/2 electron spin are given by eqs 1a and 1b[50]

$$\nu_{||\alpha(\beta)} = -\nu_I \pm \frac{(A_{iso} + 2T)}{2} \tag{1a}$$

$$\nu_{\perp\,\alpha(\beta)} = -\nu_I \pm \frac{(A_{iso} - T)}{2} \tag{1b}$$

The cross peaks for a weak hyperfine interaction are centered near the Larmor frequency (ν_I) of the nucleus such that $(\nu_\alpha + \nu_\beta)/2 \approx \nu_I$ can be used to identify the nucleus. The hyperfine coupling constant (A) of the nucleus can be estimated using the relationship $(\nu_\alpha - \nu_\beta) \approx A$. Peaks that appear along the diagonal are due to weakly coupled nuclei with $A \approx 0$. The powder line shape for an $I = 1/2$ nucleus with an axial hyperfine interaction is a narrow, curved arc extending from ($\nu_{||\alpha}$, $\nu_{||\beta}$) to ($\nu_{\perp\alpha}$, $\nu_{\perp\beta}$) along the path given by eq 2.[50,53,54]

$$\nu_\alpha = \{Q_\alpha \nu_\beta^2 + G_\alpha\}^{1/2}$$

where

$$Q_\alpha = \frac{T + 2A_{iso} - 4\nu_I}{T + 2A_{iso} + 4\nu_I} \quad (2)$$

$$G_\alpha = 2\nu_I \frac{(4\nu_I^2 - A_{iso}^2 + 2T^2 - A_{iso}T)}{T + 2A_{iso} + 4\nu_I}$$

Equation 2 shows that when ν_α^2 is plotted against ν_β^2 a straight line results with a slope and an intercept of Q_α and G_α, respectively, which can be used to determine A_{iso} and T.[50,53−55]Alternately, the frequencies at the principal values of the hyperfine tensor occur where the straight line crosses the parabola defined by $\nu_\alpha + \nu_\beta = 2\nu_I$.

For nuclei with $I = 1$, such as nitrogen, the HYSCORE spectra are much more complicated because there are more m_I states and there is also a quadrupole moment. For nitrogen-14, there are 3 nuclear frequencies in each electron spin manifold and 18 possible correlation peaks between the frequencies from different electron spin manifolds.[50,53,54] When the nitrogen hyperfine coupling is large compared to the nitrogen nuclear Zeeman and quadrupole interactions, strong modulations are observed at the nitrogen double-quantum frequencies ($\nu_{DQ\pm}$). In the HYSCORE experiment, the double-quantum features appear as cross peaks in the [±] quadrant. These are the major features due to nitrogen that are observed in this study.

HYSCORE Spectra of Hydrated Vanadium Exchanged Zeolites. Figure 1 shows the contour plot of the high-frequency region of the HYSCORE spectrum for hydrated vanadium-exchanged ZSM-5. A proton ridge is centered at approximately 15 MHz, the proton Larmor frequency. Four inequivalent protons contribute to the proton ridge and appear as four overlapping sets of ridges for hydrated VO^{2+}−ZSM-5 as illustrated in Figure 1 by the solid, dashed, and dotted lines. Proton hyperfine coupling constants are obtained via the method described by Dikanov and Bowman[50,53,54] from the coordinates (ν_α,ν_β) along each of the proton ridges as illustrated in Figure 1. A plot of ν_α^2 versus ν_β^2 is shown in Figure 2 for each of the four proton ridges of hydrated VO^{2+}−ZSM-5. The graph in Figure 2 contains both a linear least-squares fit to each set of combined data points and a curve defined by the equation $\nu_\alpha + \nu_\beta = 2\nu_I$. The points at which the extrapolated fit lines cross the curve ($\nu_\alpha + \nu_\beta = 2\nu_I$) are the ENDOR frequencies ($\nu_{\alpha,\beta}$) at the principle values of the hyperfine tensor.[50,53,54]

The principal ENDOR frequencies obtained from the data in Figures 1 and 2 are listed in Table 1. From the principal ENDOR frequencies, one can determine the principal values of the hyperfine tensor using the relationship $|(\nu_\alpha - \nu_\beta)| = |\mathbf{A}|$. However, because of ambiguities in the sign and orientation, several combinations are possible; for example, for proton A of VO^{2+}−ZSM-5, the principal values of the **A** tensor are ±6.6 and ∓4.8 MHz. To determine A_{iso} and T, we must consider four possible combinations of the **A** tensor: (−4.8, −4.8, 6.6), (6.6, 6.6, −4.8), (4.8, 4.8, −6.6), and (−6.6, −6.6, 4.8). These four combinations give possible (A_{iso}, T) values of ±(−1.0, 3.8) or ±(2.8, −3.8) MHz.

The experimental single-crystal ENDOR data[14,57] for $[VO(H_2O)_5]^{2+}$ and the quantum chemical calculations[14] provide guidance for determining which combinations of A_{iso} and T are physically realistic. The quantum calculations and the single-crystal ENDOR data for $[VO(H_2O)_5]^{2+}$ both show that the parallel value of the hyperfine coupling constant is large and positive; thus, the larger of the principal values in Table 1 was assigned as parallel with a positive sign, and the remaining value was assigned as perpendicular with the appropriate sign required by the principal values of the hyperfine tensor. Following these guidelines, $A_{iso} = -1.0$ MHz and $T = 3.8$ MHz for proton A in hydrated VO^{2+}−ZSM-5. The isotropic and dipolar coupling constants were then determined from the individual tensors and are listed in Table 1.

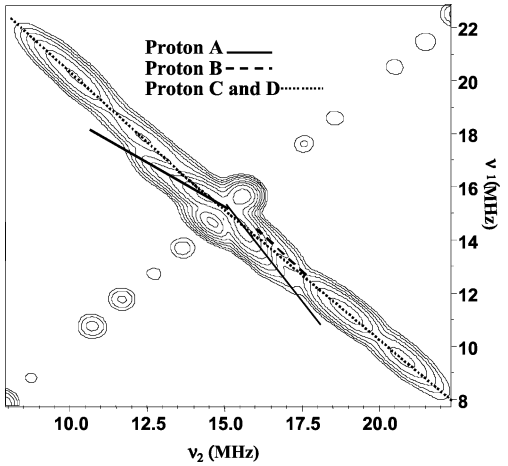

Figure 1. High-frequency region of HYSCORE spectrum 1 of hydrated VO^{2+}−ZSM-5 showing the proton ridge. This spectrum is composed of four overlapping ridges as indicated by the solid, dashed, and dotted lines, each corresponding to a different proton A, B, and C and D. The spectrum was measured at a temperature of 20 K. The microwave frequency was 9.717 GHz, and the magnetic field was 3460 G. The pulse sequence parameters were as follows: pulse 1 = 24 ns, pulses 2 and 4 = 16 ns, pulse 3 = 24 ns, step = 16 ns, τ = 160 ns, repetition rate ≈ 1 kHz, shots per loop = 64, and the number of scans of each four step cycle = 1.

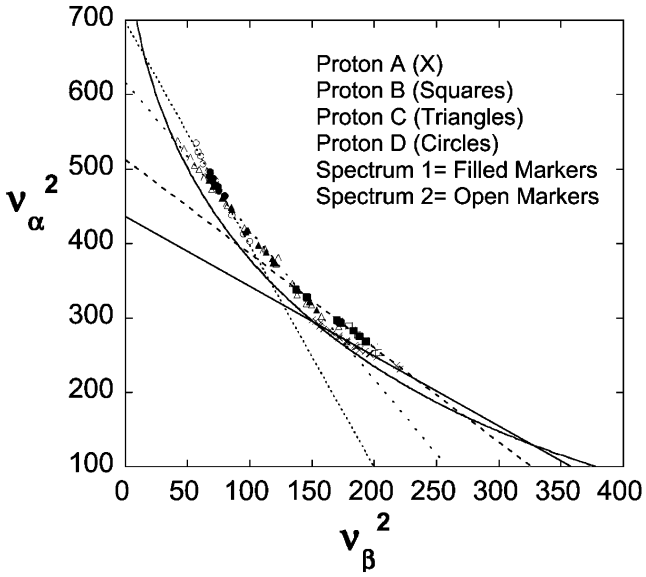

Figure 2. Analysis of protons present in the HYSCORE spectra (obtained at field values of 3460 and 3440 G) of hydrated VO^{2+}−ZSM-5. The $\nu_{\alpha,\beta}$ values determined from the proton cross peaks for each of the three protons (A, B, and C and D) are plotted as ν_α^2 vs ν_β^2. The straight lines indicate the linear least-squares fits to the plotted data points for each of the protons. The curved line is defined by $|\nu_\alpha + \nu_\beta| = 2\nu_I$. The intersections of the curved line with each of the fit straight lines represent the ENDOR frequencies of the protons.

In the single-crystal ENDOR study, Atherton and Shackleton found that two equatorial water molecules (17 and 18) in $[VO(H_2O)_5]^{2+}$ were oriented in the equatorial plane and that the other two equatorial water molecules (19 and 20) were oriented perpendicular to the equatorial plane.[57] The water molecules that were located in the equatorial plane are approximately equivalent and have a large, positive A_{iso} ranging from ∼7 to

TABLE 1: Proton Isotropic and Anisotropic (A_{iso}, T) Hyperfine Coupling Constants and Structural Assignments Determined from HYSCORE Spectra for Hydrated Vanadium-Exchanged ZSM-5 and Mordenite

	principal ENDOR frequencies (MHz)		principal values, A (MHz)		A_{iso} (MHz)	T (MHz)	assignment
V−ZSM-5							
proton A	(18.0, 11.4)	(12.3,17.1)	±6.6	∓4.8	−1.0	3.8	eq. H_2O (||)[a]
proton B	(16.5, 12.9)	(9.5, 19.9)	∓3.6	±10.4	1.1	4.7	eq. H_2O (||)[a]
proton C	(13.4 16.1)	(6.3, 23.2)	±2.7	±16.9	7.4	4.7	eq. H_2O (⊥)[b]
proton D	(10.8 18.65)	(3.9, 25.5)	±7.8	±21.6	12.4	4.6	eq. H_2O (⊥)
ammonia on VO^{2+}−ZSM-5							
proton A	(8.6, 20.8)	(13.9, 15.6)	±12.2	±1.7	5.2	3.5	
proton B	(10.6,18.8)	(14.6, 14.9)	±8.2	±0.2	2.9	2.7	
proton C	(20.6, 8.9)	(13.6,15.8)	±11.8	∓2.2	2.5	4.6	

[a] Equatorial water molecule is oriented parallel to the equatorial plane. [b] Equatorial water molecule is oriented perpendicular to the equatorial plane.

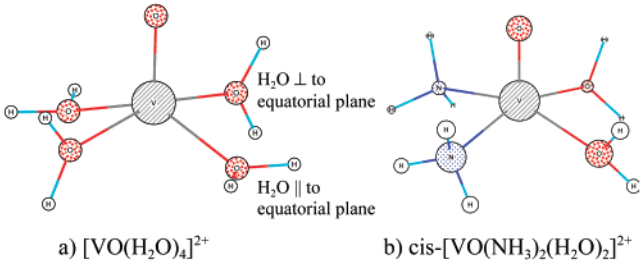

Figure 3. Proposed structures for the vanadyl complexes formed in the zeolites: (a) hydrated $[VO(H_2O_4]^{2+}$ with two water ligands oriented parallel to the equatorial plane and two water ligands oriented perpendicular to the equatorial plane and (b) mixed ammonia/water complex *cis*-$[VO(NH_3)_2(H_2O)_2]^{2+}$.

8.5 MHz and T values ranging from ∼4.75 to 5 MHz. The water molecules that were oriented perpendicular to the equatorial plane have inequivalent protons with $A_{iso} \approx 0$ and 4 MHz and T values of ∼4.5 and 5 MHz. As illustrated by these single-crystal ENDOR results, the isotropic hyperfine coupling constants of the water molecule protons are very sensitive to orientation. Recent density functional theory (DFT) calculations[14] of the proton hyperfine coupling constants for $[VO(H_2O)_5]^{2+}$ similarly demonstrate the dependence of the isotropic coupling constants upon the angle of rotation of the equatorial waters in $[VO(H_2O)_5]^{2+}$.

By correlating the HYSCORE results with the experimental and computational results, the orientations of the protons bound to the vanadium centers in the form of equatorial water were assigned as either being in the equatorial plane or perpendicular to it. As summarized in Table 1, protons A and B of VO^{2+}−ZSM-5 are assigned to the water molecules that were oriented with the protons parallel to the equatorial plane, and protons C and D are assigned to water molecules that were oriented with the protons perpendicular to the equatorial plane. These results are consistent with the single-crystal ENDOR results that suggested orientations similar to those reported here for the four equatorial water molecules in a $[VO(H_2O)_5]^{2+}$ single crystal. DFT calculations of a $[VO(H_2O)_5]^{2+}$ model complex support the conclusion that there are two water molecules that were oriented parallel to the equatorial plane and two water molecules that were oriented perpendicular to the equatorial plane. A proposed structure for the VO^{2+} complex in ZSM-5 is illustrated in Figure 3a. The similarity of the VO^{2+}−aquo complex structures to the VO^{2+}−ZSM-5 complex and to related model complexes suggests that the structure of the zeolite-bound complex is not strongly influenced by the zeolite environment for this system. The proton hyperfine coupling constants measured here by HYSCORE spectroscopy provide direct evidence of the orientation of the equatorial water ligands in VO^{2+}-exchanged zeolites. These results are supported by previous single-crystal ENDOR results and previous DFT calculations for related complexes.

HYSCORE Spectra of Vanadium-Exchanged Zeolites with Adsorbed Ammonia. The low-frequency part of the HYSCORE spectra of VO^{2+}−ZSM-5 with adsorbed ammonia is shown in Figure 4. The spectrum contains nitrogen double-quantum peaks centered at approximately (−7, 3) and (−3, 7) MHz and a proton ridge (not shown) centered at approximately 15 MHz. The proton ridge was analyzed in the same manner as the hydrated samples, and the results are listed in Table 1. For comparison with the experimental data, the results of the DFT calculations (Amsterdam Density Functional (ADF) software package) for the model vanadyl complexes with water and ammonia ligands ($[VO(NH_3)_4]^{2+}$, *cis*-$[VO(NH_3)_2(H_2O)_2]^{2+}$, *trans*-$[VO(NH_3)_2(H_2O)_2]^{2+}$, and $[VO(H_2O)_4]^{2+}$) are listed in Table 2.[15] The assignment of the proton hyperfine coupling constants to ammonia or water ligands is problematic because of the similarity of the hyperfine coupling constants for ammonia and water ligands. The earlier CW EPR and DFT calculations suggest that the ammonia complex formed in the VO^{2+} zeolites has two water and two ammonia ligands.[15] However, the computational results indicate that the proton hyperfine coupling constants for ammonia and water ligands have similar ranges, making it too difficult to assign couplings on the basis of the experimental results presented here.

The HYSCORE spectra shown in Figure 4 were obtained in the center of the vanadyl EPR line, which is not strongly orientationally selective. The dominant nitrogen modulations are due to the double-quantum transitions that are indicated in Figure 4. In the orientationally nonselective case, if the nitrogen coupling constant is assumed to be isotropic, then the frequencies of the nitrogen double-quantum peaks and eq 3 can be used to determine A_{iso} and the quadrupole coupling constant K, where $K = e^2qQ/4$.[28,58]

$$\left(\frac{\pm\nu_{dq}^2}{4}\right) - \nu_I^2 = \mp A_{iso}\nu_I + \frac{A_{iso}^2}{4} + K^2(3+\eta^2) \qquad (3)$$

The nitrogen isotropic hyperfine coupling constant (absolute values) for ammonia adsorbed on VO^{2+}−ZSM-5 was determined to be 4.8 MHz using eq 3. The A_{iso} value that was determined from the HYSCORE data for ammonia on VO^{2+}−ZSM-5 agrees very well with previous experimental results in the literature for complexes containing amine ligands on vanadyl centers. Fukui, Nishiguchi, and Kamada reported A_{iso} values of 5.1 and 5.0 MHz for the equatorially bound nitrogen model complexes $VO(gly)_2$ and VO(edda), respectively.[49] For ammonia

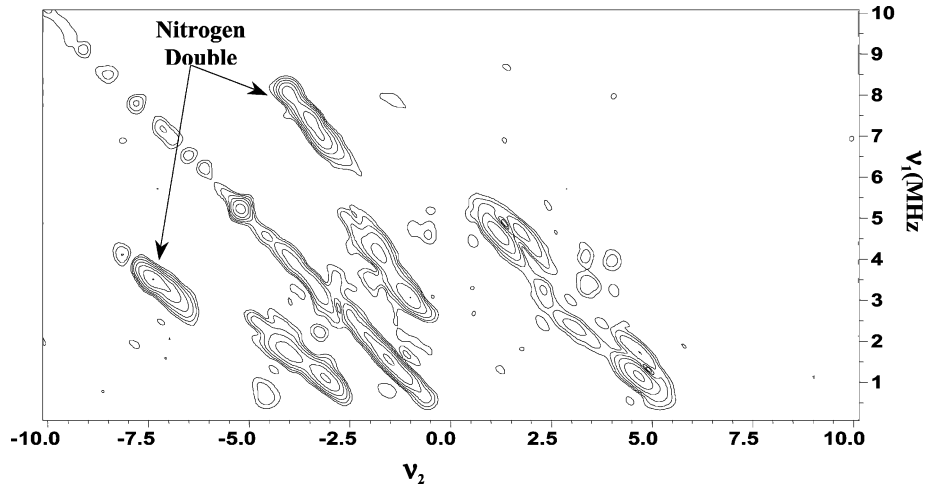

Figure 4. HYSCORE spectrum of hydrated VO^{2+}−ZSM-5 with ammonia adsorbed that was obtained at a temperature of 15 K (ν_{EPR} = 9.738 GHz, B = 3460 G). The pulse sequence parameters were as follows: pulse 1 = 24 ns, pulses 2 and 4 = 16 ns, pulse 3 = 24 ns, step = 24 ns, τ = 272 ns, repetition rate ≈ 1 kHz, shots per loop = 64, and the number of scans of each four step cycle = 1.

TABLE 2: Results of DFT Calculations for Vanadyl Model Complexes[a,b]

	principal values of A (^{14}N)	A_{iso} (^{14}N)	principal values of A (^{1}H)	A_{iso} (^{1}H)	K
$[VO(NH_3)_4]^{2+}$	5.9, 5.7, 6.2	5.8	−3.8, −2.0, 10.02 (NH_3)	1.4 (NH_3)	0.35
			8.5, 9.2, 20.1 (NH_3)	12.6 (NH_3)	
cis-$[VO(NH_3)_2(H_2O)_2]^{2+}$	5.9, 5.7 (5.6),[c] 6.2	5.9	−2.2, −0.4, 11.8 (NH_3)	3.1 (NH_3)	0.34
			3.4, 4.5, 16.0 (NH_3)	7.9 (NH_3)	
			11.7, 12.2, 23.4 (NH_3)	15.8 (NH_3)	
			−5.7, −4.9, 7.3 (H_2O)	−1.1 (H_2O)	
			−1.6, −0.9, 10.5 (H_2O)	2.6 (H_2O)	
trans-$[VO(NH_3)_2(H_2O)_2]^{2+}$	5.5, 5.9, 6.1	5.8	−3.6, −1.9, 9.7 (NH_3)	1.4 (NH_3)	0.32
			8.3, 9.0, 20.3 (NH_3)	12.5 (NH_3)	
			6.5, 6.8, 19.4 (H_2O)	10.9 (H_2O)	
$VO(H_2O)_4^{2+}$(C_{2v})			−8.4, −7.1, 4.7 (H_2O)	−3.6 (H_2O)	
			−7.1, −5.9, 6.7 (H_2O)	−2.1 (H_2O)	
			5.1, 5.4, 18.0 (H_2O)	9.5 (H_2O)	

[a] Results are from ADF calculations of model complexes reported in ref 4. [b] All values are given in MHz. [c] Principal value of nitrogen hyperfine coupling tensor for slightly inequivalent nitrogen.

adsorbed on a silica-supported vanadium oxide catalyst, the value of A_{iso} = 4.7 MHz was observed by ESEEM spectroscopy.[28]

Using eq 3, $K^2(3 + \eta^2)$ is also calculated; therefore, a range of K values corresponding to η taking on a value between 0 and 1 can be determined. The K values for ammonia adsorbed on VO^{2+}−ZSM-5 lie between 0.5 and 0.58 MHz. Literature values for K, such as 0.7 MHz for ammonia adsorbed on silica-supported vanadium oxide and 0.68 MHz for $VO(gly)_2$,[28,49] are slightly higher than the experimental values reported here. Because quadrupole coupling constants are sensitive to changes in symmetry and hydrogen bonding, the discrepancy between the results reported here and the previous results on model complexes suggests that the electronic environment of the vanadyl ammonia complex in the zeolite is slightly different than that in the model complexes.

The nitrogen hyperfine coupling constants can be compared to the computational results listed in Table 2 for the VO^{2+} model complexes with ammonia ligands. The calculated values for A_{iso} range from 5.8 to 5.9 MHz for the model complexes listed in Table 2, which are higher than the experimental values. However, the calculated values do indicate that the nitrogen hyperfine anisotropy is small, ∼0.1 to 0.2 MHz, relative to the isotropic hyperfine coupling constants for the model complexes. HYSCORE spectra (not shown) were also acquired at the parallel edge of the EPR spectrum. In this case, the spectrum is orientationally selective for parallel orientations, and eq 4 can be used to determine the parallel component of the nitrogen hyperfine coupling constant $A_{||}$ from the double-quantum frequencies.[23,47]

$$A_i = \frac{2\nu_I(\nu_{dq+} + \nu_{dq-})}{[8\nu_I - (\nu_{dq+} - \nu_{dq-})]} \qquad (4)$$

Using eq 4 and the double-quantum frequencies [±7.0, ∓3.6], $A_{||}$ is determined to be 5.0 MHz. This is very close to the A_{iso} value of 4.8 MHz, indicating that the hyperfine anisotropy in the nitrogen hyperfine interaction is very small, ∼0.1 MHz, as suggested by the computational results.

Implications of HYSCORE Results for Catalytic Applications. The vanadium-exchanged zeolites investigated in this study have been shown to be active for the SCR of NO with NH_3 according to the following reaction

$$4NO + 4NH_3 + O_2 \rightarrow 4N_2 + 6H_2O \qquad (5)$$

Previous catalytic studies of VO^{2+}-exchanged ZSM-5 indicated that the isolated VO^{2+} sites were the active sites for SCR of NO with NH_3.[5] This result was surprising because it was expected that vanadium oxide clusters would be the active sites for catalysis. The experimental HYSCORE results presented here elucidate the structures of the hydrated vanadyl and ammonia vanadyl complexes in vanadium-exchanged zeolites.

Both of these complexes are potentially important in the SCR of NO with NH_3 on vanadium-exchanged zeolites as indicated by eq 5.

As discussed in a previous section, the HYSCORE results presented here strongly suggest that the hydrated vanadyl complex in the zeolite is structurally similar to $[VO(H_2O)_5]^{2+}$; consequently, the zeolite framework does not strongly influence the structure of the hydrated vanadyl complex. Through the analysis of the HYSCORE data, the orientations of the four equatorial water ligands (two water molecules oriented perpendicular and two water molecules oriented parallel relative to the equatorial plane) were determined, as shown in Figure 3a. When the hydrated vanadium-exchanged zeolite is exposed to ammonia, strong nitrogen modulation signals appeared in the HYSCORE spectra, which were analyzed to determine the nitrogen ligand hyperfine and quadrupole interactions. The results reported here indicate that the ammonia binds in the equatorial plane with hyperfine and quadrupole coupling constants similar to those in the literature for similar complexes. Importantly, the ammonia displaces water ligands, indicating that the ammonia binds strongly to the vanadyl center in the zeolite, which is crucial for the SCR reaction because water is a product of the reaction. However, a previous EPR study suggests that the complex contains water and ammonia ligands as shown by the structure in Figure 3b. The proton hyperfine couplings of the water and ammonia ligands are too close to differentiate from one another on the basis of the results reported here.

Conclusions

HYSCORE experiments were used to measure ligand hyperfine coupling constants for water and ammonia ligands in VO^{2+}−ZSM-5. Detailed structural information about the location and orientation of the water ligands was obtained from an analysis of the HYSCORE data. The results indicated that the VO^{2+}−aquo complex that formed in the hydrated zeolites has equatorial water ligands oriented perpendicular and parallel to the equatorial plane, similar to $[VO(H_2O)_5]^{2+}$ in single crystals.[14,57] The ammonia complex that formed upon binding to the vanadium center in the exchanged zeolites was also characterized using HYSCORE spectroscopy, but the proton hyperfine coupling constants due to ammonia versus water were difficult to differentiate. The nitrogen hyperfine coupling constant was measured and assigned to an equatorial ammonia ligand.

Acknowledgment. S.L. acknowledges support from the NSF (CHE-0204847). The pulsed EPR experiments were performed in the Environmental Molecular Sciences Laboratory (a national scientific user facility sponsored by the U.S. DOE Office of Biological and Environmental Research) located at Pacific Northwest National Laboratory, operated by Battelle for the DOE. We thank A. Astashkin for the very useful method for shifting the coherent noise peaks from the pulse programmer.

References and Notes

(1) Whittington, B. I.; Anderson, J. R. *J. Phys. Chem.* **1993**, *97*, 1032.
(2) Blasco, T.; Fernandez, L.; Martinez-Arias, A.; Sanchez-Sanchez, M.; Conception, P.; Nieto, J. M. L. *Microporous Mesoporous Mater.* **2000**, *39*, 219.
(3) Petras, M.; Wichterlova, B. *J. Phys. Chem.* **1992**, *96*, 1805.
(4) Prakash, A. M.; Kevan, L. *J. Phys. Chem. B* **2000**, *104*, 6860.
(5) Wark, M.; Bruckner, A.; Liese, T.; Grunert, W. *J. Catal.* **1998**, *175*, 48.
(6) Berndt, H.; Martin, A.; Bruckner, A.; Schreier, E.; Muller, D.; Kosslick, H.; Wolf, G.-U.; Lucke, B. *J. Catal.* **2000**, *191*, 384.
(7) Mathieu, M.; Van Der Voort, P.; Weckhuysen, B. M.; Rao, R. R.; Catana, G.; Schoonheydt, R. A.; Vansant, E. F. *J. Phys. Chem B* **2001**, *105*, 3393.
(8) Chasteen, N. D. Vanadyl(IV) EPR Spin Probes: Inorganic and Biochemical Aspects. In *Biological Magnetic Resonance*; Berliner, L. J., Reuben, J., Eds.; Plenum: New York, 1981; Vol. 3; p 53.
(9) Grant, C. V.; Cope, W.; Ball, J. A.; Maresch, G. G.; Gaffney, B. J.; Fink, W.; Britt, R. D. *J. Phys. Chem. B* **1999**, *103*, 10627.
(10) Aznar, C. P.; Deligiannakis, Y.; Tolis, E. J.; Kabanos, T.; Brynda, M.; Britt, R. D. *J. Phys. Chem. A* **2004**, *108*, 4310
(11) Prakash, A. M.; Kevan, L. *J. Phys. Chem. B* **1999**, *103*, 2214.
(12) Moudrakovski, I. L.; Sayari, A.; Ratcliffe, C. I.; Ripmeester, J. A.; Preston, K. F. *J. Phys. Chem.* **1994**, *98*, 10895.
(13) Martini, G.; Ottaviani, M. F.; Seravalli, G. L. *J. Phys. Chem.* **1975**, *79*, 1716.
(14) Larsen, S. C. *J. Phys. Chem. A* **2001**, *105*, 8333.
(15) Carl, P. J.; Isley, S. L.; Larsen, S. C. *J. Phys. Chem. A* **2001**, *105*, 4563.
(16) Saladino, A. C.; Larsen, S. C. *J. Phys. Chem. A* **2003**, *107*, 1872.
(17) Saladino, A. C.; Larsen, S. C. *J. Phys. Chem. A* **2002**, *106*, 10444.
(18) Munzarova, M. L.; Kaupp, M. *J. Phys. Chem. B* **2001**, *105*, 12644.
(19) Eaton, S. S.; Eaton, G. R. In *Vanadium in Biological Systems*; Chasteen, N. D., Ed.; Kluwer Academic Publishers: Dordrecht, The Netherlands, 1990; p 199.
(20) Eaton, S. S.; Dubach, J.; More, K. M.; Eaton, G. R.; Thurman, G.; Ambruso, D. R. *J. Biol. Chem.* **1989**, *264*, 4776.
(21) Chasteen, N. D. Vanadium-Protein Interactions. In *Vanadium and Its Role in Life*; Sigel, H., Sigel, A., Eds.; Marcel Decker: New York, 1995; Vol. 31, p 231.
(22) Hamstra, B. J.; Houseman, A. L. P.; Colpas, G. J.; Kampf, J. W.; LoBrottu, R.; Frasch, W. D.; Pecoraro, V. L. *Inorg. Chem.* **1997**, *36*, 4866.
(23) Dikanov, S. A.; Tyryshkin, A. M.; Hutterman, J.; Bogumil, R.; Witzel, H. J. *J. Am. Chem. Soc.* **1995**, *117*, 7.
(24) de Boer, E.; Keijzers, C. P.; Reijerse, E. J.; Collison, D.; Garner, C. D.; Wever, R. *FEBS Lett.* **1988**, *235*, 93.
(25) Petersen, J.; Hawkes, T. R.; Lowe, D. J. *J. Am. Chem. Soc.* **1998**, *120*, 10978.
(26) Petersen, J.; Hawkes, T. R.; Lowe, D. J. *J. Inorg. Biochem.* **2000**, *80*, 161.
(27) Gerfen, G. J.; Hanna, P. A.; Chasteen, N. D.; Singel, D. J. *J. Am. Chem. Soc.* **1991**, *113*, 9513.
(28) Larsen, S. C.; Singel, D. J. *J. Phys. Chem.* **1992**, *96*, 9007.
(29) van Willigen, H.; Chandrashekar, T. K. *J. Am. Chem. Soc.* **1983**, *105*, 4232.
(30) *ESEEM of Nitrogen Coordinated Oxo-Vanadium(IV) Complexes* Riejerse, E. J.; Shane, J., de Boer, E., Collison, D., Eds.; World Scientific Publishers: Singapore City, Singapore, 1989.
(31) Mulks, C. F.; Kirste, B.; van Willigen, H. *J. Am. Chem. Soc.* **1982**, *104*, 5906.
(32) Mulks, C. F.; van Willigen, H. *J. Phys. Chem.* **1981**, *85*, 1220.
(33) LoBrutto, R.; Hamstra, B. J.; Colpas, G. J.; Pecoraro, V. L.; Frasch, W. D. *J. Am. Chem. Soc.* **1998**, *120*, 4410.
(34) Anderson, M. W.; Kevan, L. *J. Phys. Chem.* **1987**, *91*, 4174.
(35) Goldfarb, D.; Kevan, L. *J. Am. Chem. Soc.* **1987**, *109*, 2303.
(36) Sass, C. E.; Kevan, L. *J. Phys. Chem.* **1989**, *93*, 7856.
(37) Lei, G.-D.; Kevan, L. *J. Phys. Chem.* **1990**, *94*, 6384.
(38) Yu, J.-S.; Kevan, L. *J. Phys. Chem.* **1990**, *94*, 7620.
(39) Kevan, L.; Yu, J.-S. Copper Ion Catalysis of Complete and Partial Oxidation of Propylene on X and Y Zeolites: Correlation of Electron Spin Resonance and Product. In *Research on Chemical Intermediates*; Elsevier Science Publishers B. V.: Amsterdam, 1991; Vol. 15, p 67.
(40) Lei, G.-D.; Kevan, L. *J. Phys. Chem.* **1991**, *95*, 4506.
(41) Finel, C.; Kevan, L. *J. Chem. Soc., Faraday Trans.* **1993**, *89*, 2559.
(42) Luan, Z.; Xu, J.; He, H.; Klinowski, J.; Kevan, L. *J. Phys. Chem.* **1996**, *100*, 19595.
(43) Kevan, L.; Prakash, A. M. *J. Phys. Chem. B* **2000**, *104*, 6860.
(44) Hofer, P.; Grupp, A.; Nebenfuhr, H.; Mehring, M. *Chem. Phys. Lett.* **1986**, *132*, 279.
(45) Carl, P. J.; Vaughan, D. E. W.; Goldfarb, D. *J. Phys. Chem. B* **2002**, *106*, 5428.
(46) Zhang, J.; Carl, P. J.; Zimmermann, H.; Goldfarb, D. *J. Phys. Chem. B* **2002**, *106*, 5382.
(47) Dikanov, S. A.; Liboiron, B. D.; Orvig, C. *J. Am. Chem. Soc.* **2002**, *124*, 2969.
(48) Buy, C.; Matsui, T.; Andrianambinintsoa, S.; Sigalat, C.; Girault, G.; Zimmermann, J. *Biochemistry* **1996**, *35*, 14281.
(49) Fukui, K.; Ohya-Nishiguchi, H.; Kamada, H. *Inorg. Chem.* **1997**, *36*, 5518.
(50) Dikanov, S. A.; Bowman, M. K. *J. Magn. Reson.* **1995**, *116*, 125.
(51) Samooilova, R. I.; Dikanov, S. A.; Fionov, A. V.; Tyryshkin, A. M.; Lunina, E. V.; Bowman, M. K. *J. Phys. Chem.* **1996**, *100*, 17621.
(52) Schweiger, A.; Jeschke, G. *Principles of Pulse Electron Paramagnetic Resonance*; Oxford University Press: New York, 2001.

(53) Dikanov, S. A.; Bowman, M. K. *JBIC* **1998**, *3*, 18.
(54) Dikanov, S. A.; Tyryshkin, A., M.; Bowman, M. K. *J. Magn. Reson.* **2000**, *144*, 228.
(55) Konovolova, T. A.; Dikanov, S. A.; Bowman, M. K.; Kispert, L. D. *J. Phys. Chem. B* **2001**, *105*, 8361.
(56) Gemperle, C.; Aebli, G.; Schweiger, A.; Ernst, R. R. *J. Magn. Reson.* **1990**, *88*, 241.
(57) Atherton, N. M.; Shackleton, J. F. *Mol. Phys.* **1980**, *39*, 1471.
(58) Dikanov, S. A.; Tsvetskov, Y. D.; Bowman, M. K.; Ashtashkin, A. V. *Chem. Phys. Lett.* **1982**, *90*, 149.